Chapter VIII

Screening of Triazine Derivatives, Inhibitors of MAP-kinase p-38 Alpha, Through Mathematical Modeling And Molecular Modeling

8.1: Introduction

The mitogen-activated protein (MAP) kinases comprise a family of serine/threonine kinases that function as critical mediators of signal transduction [1-3]. So far, four different MAP-kinases have been described: the extracellular signal-related kinases (ERKs), the c-Jun N-terminal kinases (JNKs), the p38 MAP-kinases and the ERK5 or big MAP kinase 1 (BMK1). The ERK MAP-kinases are preferentially activated by mitogens, whereas the JNK and p38 MAP-kinases are responsive to stress and inflammatory signals and it is also an important mediator of anti-estrogen growth inhibition in breast cancer [4].

Tamoxifen was shown to activate JNK and p38 MAP-kinases in connection with programmed cell death [5,6]. However, tamoxifen induced apoptosis occurs only at high concentrations and seems to be ER independent as it is not reversible by addition of estradiol [7] and it is also seen that breast tumor often becomes resistant to tamoxifen. This necessitates looking for other inhibitors for P38 MAP kinase for cancer therapy. Triazines might be a good candidate as it is reported to have antitumoral activities [8].Hexamethylmelamine (HMM), a derivative of triazine-A (Figure 1) possess various pharmacological actions against breast, lung and ovarian cancers, but once again causes nausea, vomiting, abdominal cramps, and anorexia. Compound B (Figure 1) was investigated by Moon et. al [9] as a microbial destabilizing agent entity with potent growth inhibition against U937cells(GI50=1μm). Leftheris et al reported compound C (Figure 1) as a potent inhibitor of p38 MAP kinase [10].

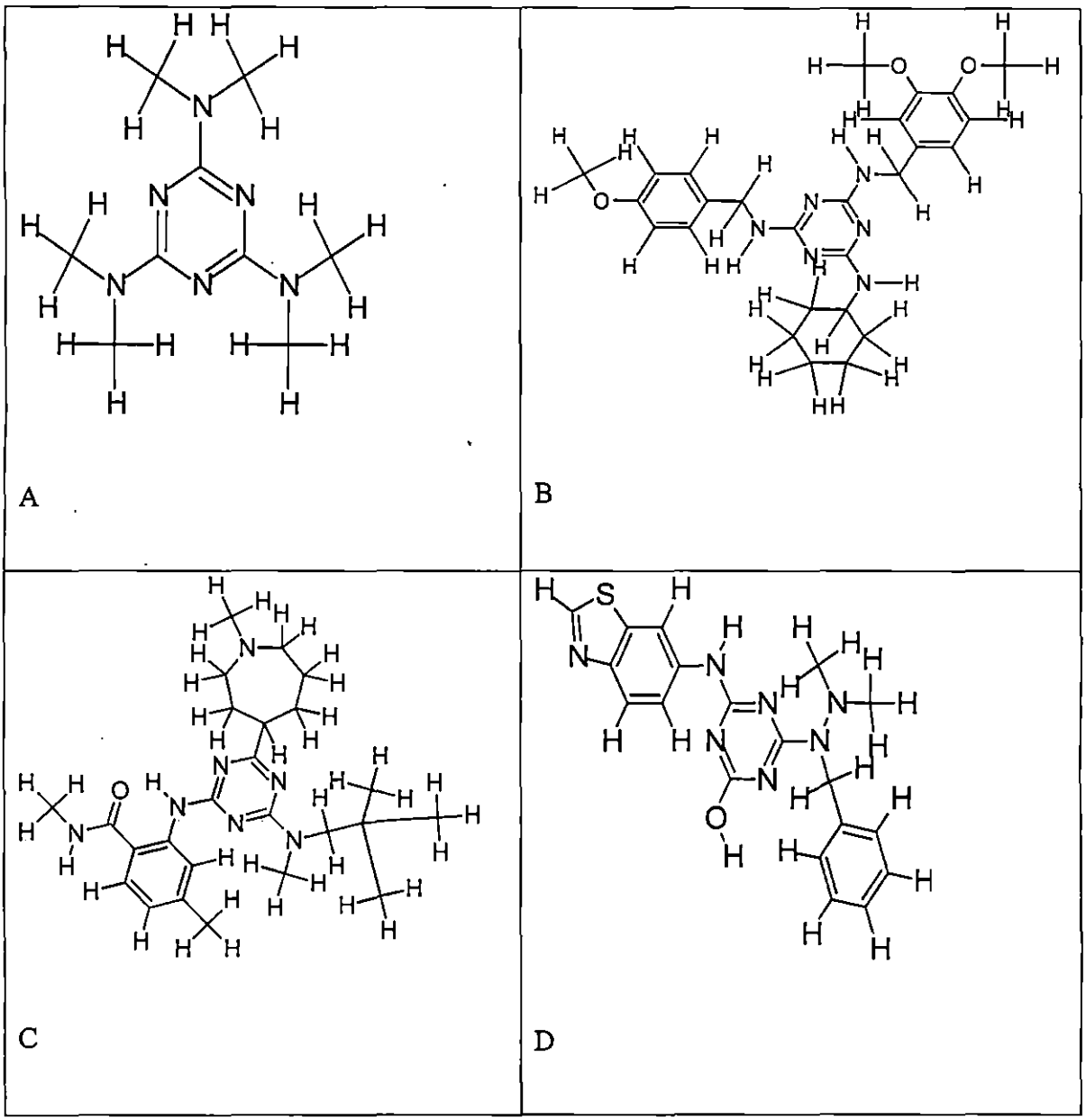

Figure 1. Reported triaminotriazine compounds with antitumor activity

Compound E (triaminotrizine derivatives) (Figure 2) was recently reported by "Baindur et al." [11] as a potent VEGF-R2 (KDR) tyrosine kinase inhibitor. It is a common feature for compounds to exhibit antitumor activities by introducing structural units of various aryl amino groups into the triazine scaffold. "Zheng et al." introduced structural units of various aryl amino groups in to the triazine scaffold and determined their biological activity [12]. Taking the experimental activity from the work of "Zheng et al." as dependent variable, we formulate a mathematical model, based on graph theoretical

indices, quantum chemical and structural parameters to design numbers of potent triazine scaffold-based inhibitor.

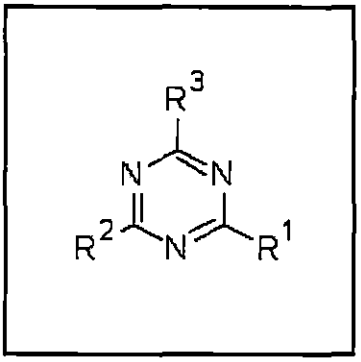

Figure 2: Structural representation triaminotrizine derivatives

An important advance in QSAR has been the application of a mathematical technique "Graph Theory" to chemistry [13]. In chemical graph theory [14], molecular structures are represented as hydrogen-suppressed graphs, commonly known as molecular graph, in which vertices and the bonds represent the atoms by edges. The connections between atoms can be described by topological matrices, which can be mathematically manipulated so as to derive a single number, known as topological index (TI) [15].

Topological indices offer a viable way of measuring molecular branching, shape and size [16]. Quantum chemical parameters like, HOMO & LUMO energy, dipole moment is also very helpful to develop the quantitative structure activity relationship.

In this communication we would like to consider different parameters and indices, namely IC (Mean Information Content), SIC (Structural Information Content), CIC (Complementary Information Content) and some quantum chemical parameters namely, HOMO, LUMO, Dipolemoment, Polarisability of the triazine derivatives [12] are calculated and a regression equation is formulated. Some chemically feasible compounds are designed and their theoretical activity is calculated and further binding energies of the

designed inhibitors were calculated through docking the inhibitors into the binding site of p-38 MAP kinase inhibitor. This will help us to screen potent inhibitors.

8.2: Materials and Methods

Biological Data and Structures

The total set of 22 triazine derivatives was divided into 16 compounds in training set and six compounds in test set on the basis of their activity against HT-29 cells. Training set of triazine derivatives (1a -1p) are shown in Table 1. For validation of the trained set, we used a test set consisting of triazine derivatives (2a – 2f) are given in Table 2.

Table 1. Chemical structures and inhibitory activities against HT-29 cells of triazine derivatives (Training set) by substituting R1, R2, R3 of E.

Compound	R1	R2	R3	%Inhibition at μM[α] HT-29
1a	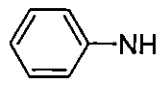	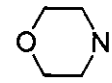	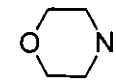	80.5
1b	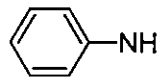	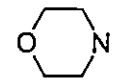	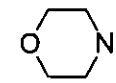	74.2
1c	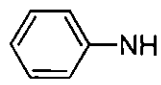	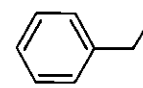	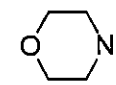	90.5
1d	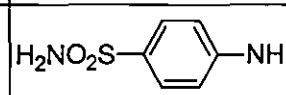	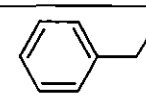	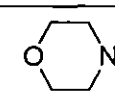	68.6
1e	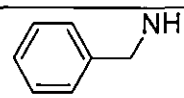	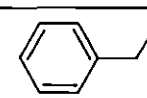	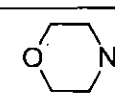	50.0

Compound	R1	R2	R3	%Inhibition at μM[α] HT-29
1f	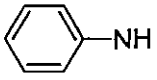	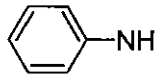	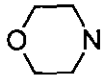	85.0
1g	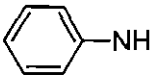	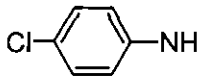	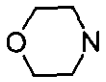	87.1
1h	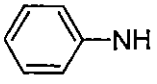	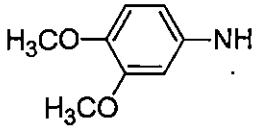	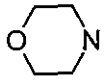	76.4
1i	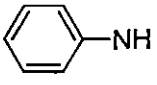	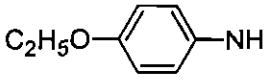	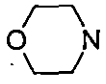	87.5
1j	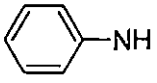	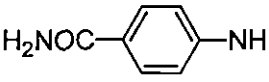	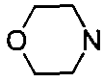	87.8
1k	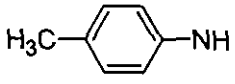	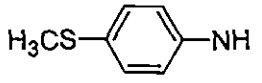	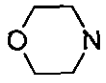	54.1
1l	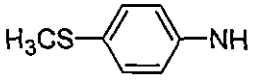	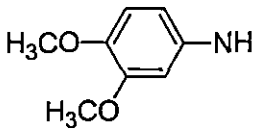	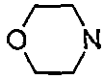	81.4
1m	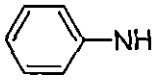	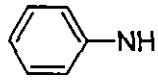	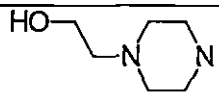	76.1
1n	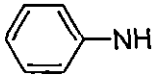	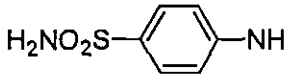	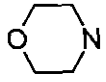	80.4
1o	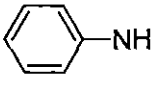	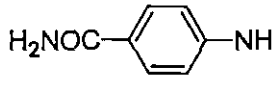	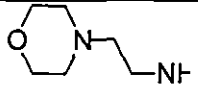	74.6
1p	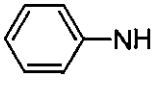	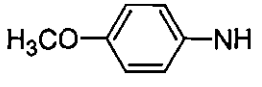	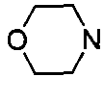	100.00

Table 2.Chemical structures and inhibitory activities against HT-29 cells of triazine derivatives (Test set) by substituting R1, R2, R3 of E.

Compound	R1	R2	R3	%Inhibition at μM[a] HT-29
2a	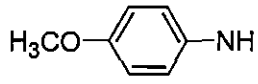	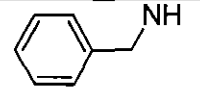	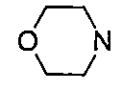	88.4
2b	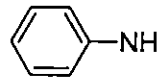	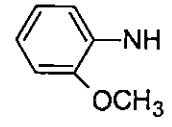	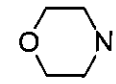	89.3
2c	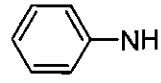	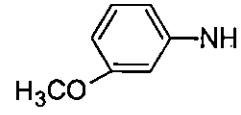	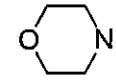	87.4
2d	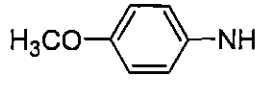	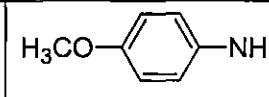	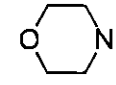	80.6
2e	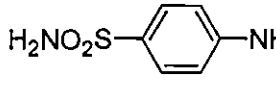	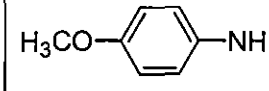	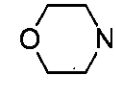	83.2
2f	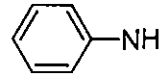	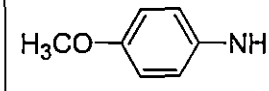	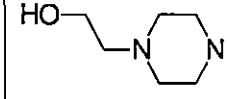	77.3

Topological Indices

A major part of the current research in COMPUTATIONAL chemistry, chemical graph theory, and quantitative structure-activity/property relationship studies involves topological indices. Topological indices (TIs) are numerical graph invariants that quantitatively characterize molecular structure.

Information theoretic topological indices are calculated by the application of information theory to chemical graphs. An appropriate set of n-elements is derived from a molecular graph G depending upon certain structural characteristics. On the basis of a equivalence

relation defined on A1, the set A is partitioned into h disjoint subsets Ai of order (i=1, 2,... $h_i \sum_{i=1}^{n} n_i = n$). A probability distribution is then assigned to the set of equivalence classes.

$$A_1, A_2, A_3, \ldots\ldots, A_h$$

$$p_1, p_2 \ldots\ldots\ldots\ldots\ldots p_h$$

Where $p_i = \frac{n_i}{n}$ is the probability that a randomly selected element of A will occur in the ith subset.

$$W(G) = \sum_{i=1}^{N} \sum_{j=i}^{N} \mathbf{D}_{ij}(G) \tag{1}$$

The mean information content of an element of A is defined by Shanon's relation [17].

$$IC = -\sum_{i=1}^{n} p_i \log_2 p_i \tag{2}$$

The logarithm is taken at base 2 for measuring the information content in bits. The total information content of the set A is then n*IC.

In this method chemical species are symbolized by weighted linear graphs. Two vertices u_0 and v_0 of a molecular graph are said to be equivalent with respect to the rth order neighborhood if and only if corresponding to each path u1,u2,....ur of length r , there is a distinct path v1,v2,.....vr of the same length ,such that the paths have similar edge weights ,and both u0 and v0 are connected to the same number and type of atoms up to the rth order bonded neighbors.

Once partitioning of the vertex set for a particular order of neighborhood is completed, ICr is calculated from the appropriate equation. Basak, Roy and Ghosh defined another information theoretic measure, Structural Information Content (SIC) [18], which is calculated as

$$SIC_r = \frac{IC_r}{\log_2 n} \tag{3}$$

Where IC is calculated from equation and n is the total number of vertices of the graph.

Another information-theoretic invariant, Complementary Information Content (CIC) (19Basak*et al.*, 1983), is defined as

$$CIC_r = \log_2 n - IC \tag{4}$$

CIC represents the difference between the maximum possible complexity of a graph (where each vertex belongs to a separate equivalence class) and the realized topological information of a chemical species as defined by ICr., HOMO, LUMO, Dipole moment, Polarisability are calculated using Mopac (20James *et al.*, 2007) and Arguslab [21].

We have taken x-ray structure of MAP kinase p-38 [22] from the protein data bank (PDB entry 1kv2) for calculating binding free energy of the designed molecules. We have performed docking by using Arguslab and obtained the binding free energy of training molecules and designed molecules.

Preparation of protein

We have taken x-ray crystal structure of the MAP kinase p-38 from the protein data bank (PDB ID: 1kv2) (http://www.pdb.org) [22]. The crystal structure of the complex of ligand with protein is available in Pdb. From this we get the binding site. Missing atoms were

repaired by the SPDBV software package and then it is minimized by steepest descent method.

Preparation of ligand

All triazine inhibitors used for docking study were collected from the published work of Zheng*et al.* []. Using draw mode of Chemsketch the ligand molecules were drawn and three dimensional optimizations were done and then saved in mol file. Geometry optimizations of the ligands were performed by ArgusLab 4.0.1 software. [21].

Docking Studies

Docking simulations were performed by selecting "ArgusDock" as the docking engine. The selected residues of the receptor were defined to be a part of the binding site. A spacing of 0.4 Å between the grid points was used and an extensive search was performed by enabling "High precision" option in Docking precision menu, "Dock" was chosen as the calculation type, "flexible" for the ligand and the AScore was used as the scoring function. The binding site box size was set to 60 x 60 x 60 Å, so as to encompass the entire active site. The AScore function, with the parameters read from the AScore.prm file, was used to calculate the binding energies of the resulting docked structures. The docking poses were saved for each compound according to their dock score function.

Computer Software

In this work different software are used like Chemsketch, Matlab-IV, Arguslab 4.01 and several program written by ourselves in Fortran-77 are used.

8.3: Results and Discussion

The values of graph theoretical indices, quantum chemical parameters and experimental HT-29 value of training set is given in Table 3 and test set is given in Table 4. Using the

parameters, multivariate regression analysis was performed with the training set and validated by test set.

Table 3. Graph theoretical indices, quantum chemical parameters, experimental activity of training set.

Compound	Homo kcal/mol	Lumo kcal/mol	Dipole moment (debye)	SIC	CIC	Polarisibility (cm^3)	%Inhibition at $_{\mu}M^a$ HT-29
1a	-0.3628	-0.0314	5.287	0.4891	2.8374	37.07	80.5
1b	-0.3528	-0.0321	5.7053	0.5012	2.8295	39.72	74.2
1c	-0.3544	-0.0262	3.4335	0.4914	2.8555	41.94	90.5
1d	-0.365	-0.0714	10.717	0.5575	2.5464	45.99	68.6
1e	-0.3548	-0.0283	3.697	0.4709	3.0161	43.81	50
1f	-0.3565	-0.0251	3.2595	0.505	2.7345	40.07	85
1g	-0.3592	-0.0295	3.4301	0.5374	2.5549	42.01	87.1
1h	-0.3445	-0.0269	4.691	0.5161	2.7846	45.36	76.4
1i	-0.3504	-0.0259	2.7284	0.503	2.8471	44.55	87.5
1j	-0.3368	-0.0218	6.6385	0.5625	2.4692	43.61	87.8
1k	-0.2963	-0.0272	2.8242	0.5335	2.672	46.07	54.1
1l	-0.2975	-0.0296	3.5978	0.5351	2.7236	49.28	81.4
1m	-0.3248	-0.0232	3.3403	0.4953	2.9044	45.15	76.1
1n	-0.3657	-0.0607	6.7406	0.5661	2.4613	44.16	80.4
1o	-0.3156	-0.0046	3.24	0.5067	2.8894	48.29	74.6
1p	-0.3547	-0.0252	4.6082	0.5164	2.7295	42.72	100

Table 4. Graph theoretical indices, quantum chemical parameters and experimental activity of test set.

Compound	Homo kcal/mol	Lumo kcal/mol	Dipole Moment (debye)	SIC	CIC	Polarisibility (cm^3)	%Inhibition at μM^{α} HT-29
2a	-0.3522	-0.0266	3.9354	0.5095	2.8095	44.59	88.4
2b	-0.3542	-0.0193	4.8844	0.5164	2.7295	42.72	89.3
2c	-0.3568	-0.0254	4.8058	0.5164	2.7295	42.72	87.4
2d	-0.3455	-0.0267	3.5659	0.5161	2.7846	45.36	80.6
2e	-0.326	-0.0593	5.7084	0.5779	2.4404	46.68	83.2
2f	-0.3495	-0.0405	5.3335	0.5171	2.8289	47.8	77.3

PRESENTATION OF QSAR MODELS

First, we have taken the SIC and CIC and constructed a regression model is given in equation 5. N is the number of compounds in training set. This equation gives moderate result with chi-square value 4.582513.

$$HT29 = 599.7415+(-480.2107)XSIC+(-99.4646)*CIC \quad (5)$$

$$N=16,\ \chi^2 = 4.582513$$

After that we took the HOMO and LUMO and constructed another regression model is given by equation 6.

$$HT29 =0.7417 +(-252.2386)XHOMO+(292.1922)LUMO \quad (6)$$

$$N=16,\ \chi^2 = 4.673094$$

These two models suggest that structural information and electronic information both are capable of providing predicted values which are not too bad. To improve the model we constructed regression model (equation 7) of comprising SIC, CIC, HOMO and LUMO which further improves the result. This is also evident from the χ^2 test which shows better result.

HT29=-160.62791 +(-0.3432) XHOMO+(-0.3057) XLUMO+(0. 51795) XSIC+ (2.740963)XCIC (7)

N=16, χ^2 = 2.851216

Lastly we inserted dipole moment and polarizability to construct a regression model with six parameters SIC, CIC, HOMO, LUMO, Dipole Moment and Polarisibility which gives very good result with chi-square value 0.99211. So the last model represented by equation 8 is very useful for screening these types of inhibitors.

HT29=-1932.1210+[(-0.5853)Homo+0.5539Lumo+(-0.0047)DM+2.3207SIC+0.3043CIC+ (-0.0045)Pol]*1000 (8)

N=16, χ^2 = 0.99211

We have applied these models to several compounds designed by ourselves and predicted their activities. Predicted HT-29 values of training set using different models are given in table 5.

Table 5: Experimental and predicted value of the compounds under training set with different models.

Compound	Experimental %Inhibition at μM[a] HT-29	Predicted %Inhibition at μM[a] HT-29 (By equation 5)	Predicted %Inhibition at μM[a] HT-29 (By equation 6)	Predicted %Inhibition at μM[a] HT-29 (By equation 7)	Predicted %Inhibition at μM[a] HT-29 (By equation 8)
1a	80.5	82.64956	83.07904	77.41712	78.64453
1b	74.2	77.62477	80.35212	76.31468	84.18933
1c	90.5	79.74475	82.47963	78.15458	74.25037
1d	68.6	78.74733	71.94627	70.93029	62.30176
1e	50	73.61508	81.96691	70.90522	64.96387
1f	85	85.24913	83.33075	83.73767	80.0625
1g	87.1	87.55414	82.72613	91.0948	90.21241
1h	76.4	74.9356	79.77793	80.65373	82.51416
1i	87.5	75.00981	81.55833	79.90289	88.0083
1j	87.8	84.02495	79.32588	94.48669	91.25818
1k	54.1	77.77965	67.53237	66.8434	65.83154
1l	81.4	71.87896	67.1338	65.9483	66.53845
1m	76.1	73.0081	75.88994	69.55018	68.51123
1n	80.4	83.08199	75.24929	80.87525	89.62232
1o	74.6	69.02569	79.00412	81.37932	81.66174
1p	100	80.27204	82.84749	86.00583	85.62427

Correlation graph of predicted values of HT-29 against experimental values of HT-29 of training set is given Figure 3. R^2 value of training set is 0.4181.

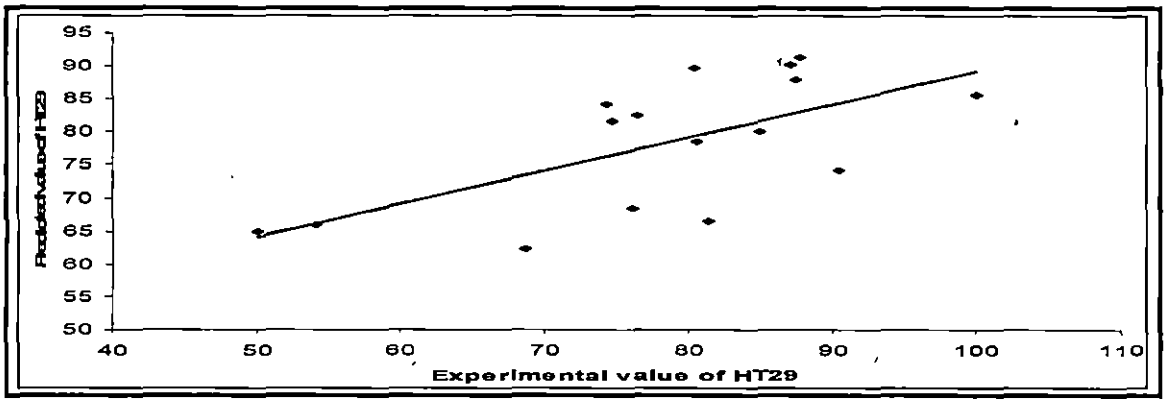

Figure 3. Correlation graph between Theoretical and predicted activity of training set

Predicted HT-29 values of test set using different models are given in table 6 and R^2_{pred} for test set using equation 8 is 0.335.

Table 6: Experimental and predicted value of the compounds under test set with different models.

compounds	Experimental %Inhibition at μM[a] HT-29	Predicted %Inhibition at μM[a] HT-29 (By equation 5)	Predicted %Inhibition at μM[a] HT-29 (By equation 6)	Predicted %Inhibition at μM[a] HT-29 (By equation 7)	Predicted %Inhibition at μM[a] HT-29 (By equation 8)
2a	88.4	75.62831	81.80782	81.99198	86.46399
2b	89.3	80.27204	84.4453	89.7197	87.30139
2c	87.4	80.27204	83.31875	86.68493	85.81385
2d	80.6	74.9356	80.0886	81.17263	88.49817
2e	83.2	79.4943	65.64448	69.65482	81.69715
2f	77.3	70.04911	77.06531	73.67898	79.70923

The structures of designed molecules with their predicted HT-29 values with the help of equation 8 are represented in Table 7. So these compounds may act as good inhibitors.

Table 7. Chemical structures of designed triazine derivatives by substituting R1, R2, R3 of E and their predicted value of HT-29 by equation 8.

Compound	R1	R2	R3	%Inhibition at μM[a]HT-29 Model 4
3a	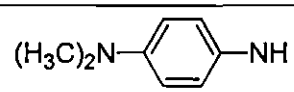	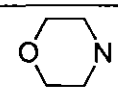	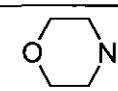	56.43
3b	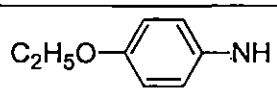	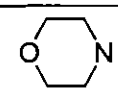	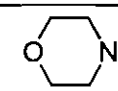	70.48
3c	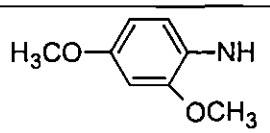	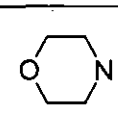	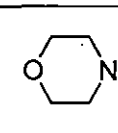	79.48

Compound	R1	R2	R3	%Inhibition at μM[α] HT-29 Model 4
3d	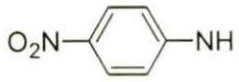		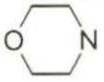	73.77
3e	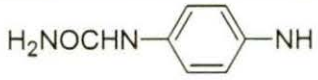	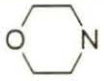	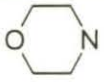	74.16
3f	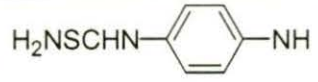	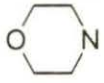	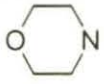	70.02
3g	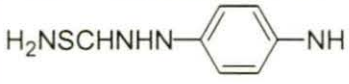	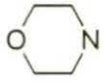	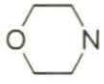	98.27
3h	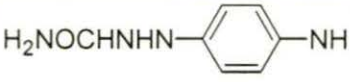	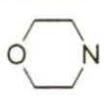	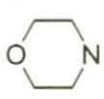	87.47
3i	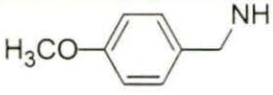	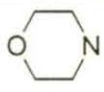	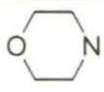	75.85
3j	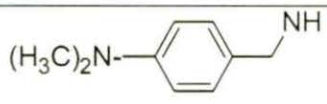	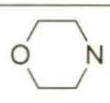	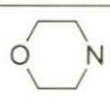	78.89
3k	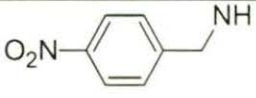	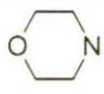	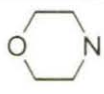	67.38
3l	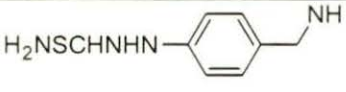	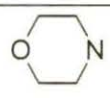	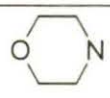	61.50
3m	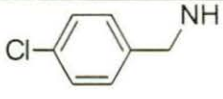	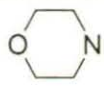	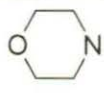	81.31
3n	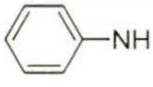	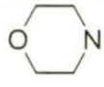	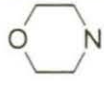	71.16
3o	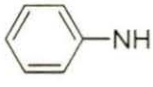	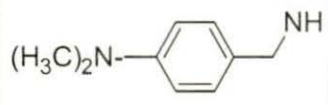	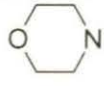	57.00

Compound	R1	R2	R3	%Inhibition at μM[c] HT-29 Model 4
3p	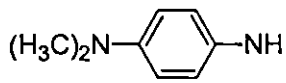	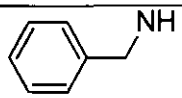	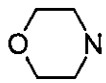	54.37
3q	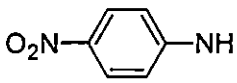	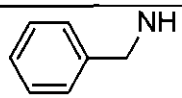	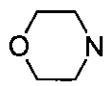	21.79
3r	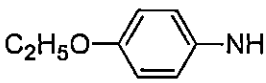	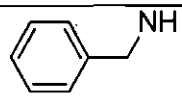	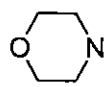	66.64
3s	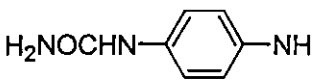	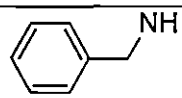	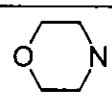	83.64
3t	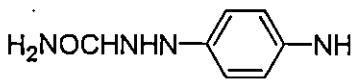	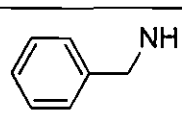	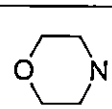	75.79
3u	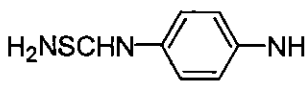	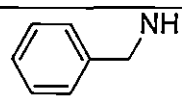	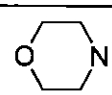	55.64
3v	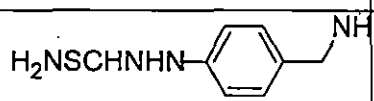	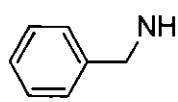	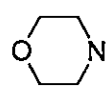	60.48
3w	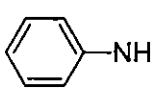	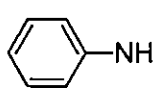	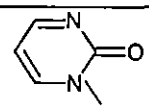	73.62
3x	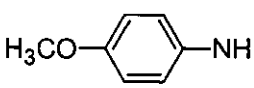	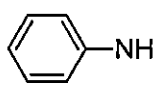	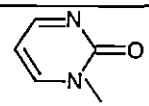	74.8
3y	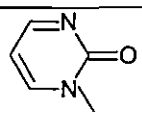	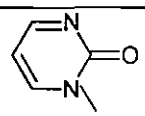	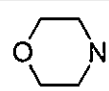	61.22

Compound	R1	R2	R3	%Inhibition at μM[a] HT-29 Model 4
3z	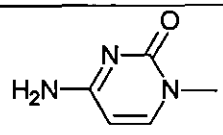	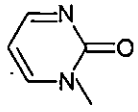	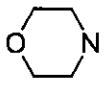	106.74
4a	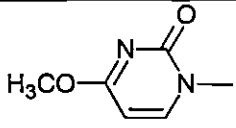	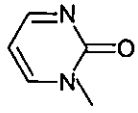	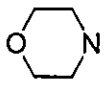	72.52
4b	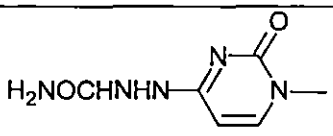	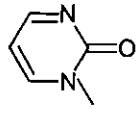	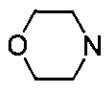	138.95
4c	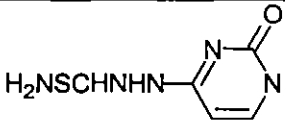	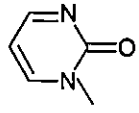	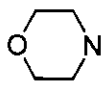	65.79
4d	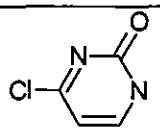	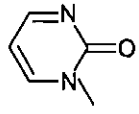	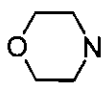	110.58
4e	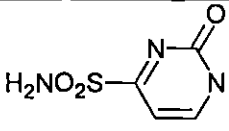	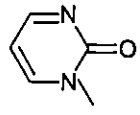	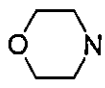	111.01
4f	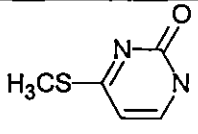	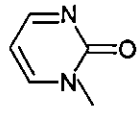	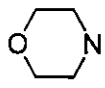	83.93
4g	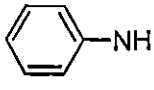	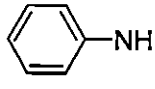	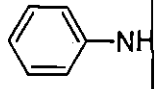	3.03
4h	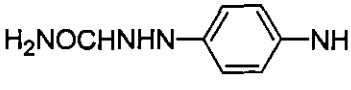	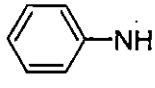	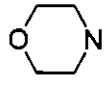	80.09

Compound	R1	R2	R3	%Inhibition at μM[α] HT-29 Model 4
4i	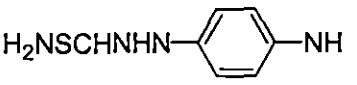	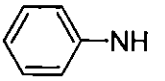	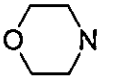	29.22

Values of graph theoretical indices, quantum chemical parameters of the designed compounds (3a-3z, 4a-4i) are represented in Table 8 and their activities are (predicted by equation 8) is given in same table.

Table 8. Graph theoretical indices, quantum chemical parameters and predicted activity of designed molecules.

Name of compound	Homo kcal/mol	Lumo kcal/mol	Dipole Moment (debye)	SIC	CIC	Polarisibility (cm^3)	Predicted %Inhibition at μM[α] HT-29 (By equation 8)
3a	-0.324	-0.0177	7.4078	0.4765	3.0268	42.74	56.43
3b	-0.3261	-0.0189	6.8958	0.4941	2.9114	41.55	70.48
3c	-0.3336	-0.0157	6.5859	0.4957	2.9157	42.36	79.48
3d	-0.3574	-0.0587	5.3187	0.5146	2.7258	39.66	73.77
3e	-0.3145	-0.0147	10.7156	0.5522	2.565	42.29	74.16
3f	-0.3139	-0.0179	8.3862	0.5522	2.565	45.17	70.02
3g	-0.3067	-0.0216	9.6827	0.6232	2.1781	46.6	98.27
3h	-0.3272	-0.0181	10.3029	0.5611	2.5374	43.72	87.47
3i	-0.3531	-0.0093	9.1175	0.4852	2.9624	41.59	75.85
3j	-0.3513	-0.0109	6.7253	0.4688	3.1117	44.62	78.89
3k	-0.3681	-0.0603	9.8262	0.5236	2.7159	41.54	67.38

Name of compound	Homo kcal/mol	Lumo kcal/mol	Dipole Moment (debye)	SIC	CIC	Polarisibility (cm^3)	Predicted %Inhibition at μM^{α} HT-29 (By equation 8)
3l	-0.3076	-0.014	9.4549	0.5433	2.6752	48.47	61.50
3m	-0.3571	-0.0125	7.8039	0.5066	2.7845	40.88	81.31
3n	-0.3123	-0.0104	4.9425	0.5161	2.7717	44.59	71.16
3o	-0.312	-0.0065	5.2811	0.486	2.9981	47.61	57.00
3p	-0.3098	-0.0034	5.9317	0.486	2.9981	47.61	54.37
3q	-0.3429	-0.0452	12.2131	0.5062	2.801	44.54	21.79
3r	-0.3122	-0.0049	6.0474	0.5055	2.872	46.42	66.64
3s	-0.3122	-0.0049	6.0474	0.5475	2.6185	47.16	83.64
3t	-0.3154	-0.0063	9.1228	0.5578	2.5792	48.59	75.79
3u	-0.3105	-0.0113	8.2818	0.5475	2.6185	50.04	55.64
3v	-0.282	-0.0029	5.7743	0.5578	2.5778	51.47	60.48
3w	-0.3241	-0.0366	5.7463	0.5771	2.2946	40.71	73.62
3x	-0.325	-0.0373	6.9574	0.5804	2.3307	43.35	74.83
3y	-0.3714	-0.0546	11.7836	0.5658	2.3106	36.35	61.22
3z	-0.3839	-0.0667	11.4005	0.6204	2.0471	37.11	106.74
4a	-0.3815	-0.0521	11.8090	0.5650	2.3939	38.66	72.52
4b	-0.3744	-0.065	7.4158	0.647	1.9715	41.7	138.95
4c	-0.2563	-0.0508	8.2841	0.6439	1.9889	43.01	65.79
4d	-0.3862	-0.0611	9.9393	0.6283	1.9781	38.18	110.58
4e	-0.3953	-0.1011	12.5408	0.6636	1.8472	40.98	111.01
4f	-0.3627	-0.0614	9.6989	0.6044	2.1595	41.2	83.93
4g	-0.3174	-0.0081	2.4132	0.4295	3.1329	43.07	3.03

Name of compound	Homo kcal/mol	Lumo kcal/mol	Dipole Moment (debye)	SIC	CIC	Polarisibility (cm^3)	Predicted %Inhibition at μM^{α} HT-29 (By equation 8)
4h	-0.3209	-0.0135	8.2205	0.563	2.5146	46.72	80.09
4i	-0.229	-0.0095	7.2959	0.5695	2.4776	48.38	29.22

We have calculated the binding free energy of the compounds 1a to 1p of training set by docking using the software Arguslab. Values of binding free energy of all the compounds under training set are given in table 9.

Table 9. Experimental value of HT-29 and binding free energy of training set.

Compound	Experimental %Inhibition at □□□ HT-29	Binding free energy in kcal/mol
1a	80.5	-5.22
1b	74.2	-6.77
1c	90.5	-9.47
1d	68.6	-9.25
1e	50	-11.66
1f	85	-7.53
1g	87.1	-8.93
1h	76.4	-7.88
1i	87.5	-7.61
1j	87.8	-9.65
1k	54.1	-11.30
1l	81.4	-8.63
1m	76.1	-8.06

1n	80.4	-9.70
1o	74.6	-7.91
1p	100	-7.94

We performed the docking of our designed molecules (3a-3z, 4a-4i) with the protein P38 map kinase (PDB 1kv2) and calculated binding free energy. It was found that the binding energy lies between –7.3578 kcal/mol (3g) to –11.7924 kcal/mol (4d), which indicates that these are favorable for binding. The correlation between exp% inhibition and free energy of binding is shown in figure 4 and Value of R^2 is 0.2607. Low value of R^2 indicates that the activity does not depend fully on binding energy

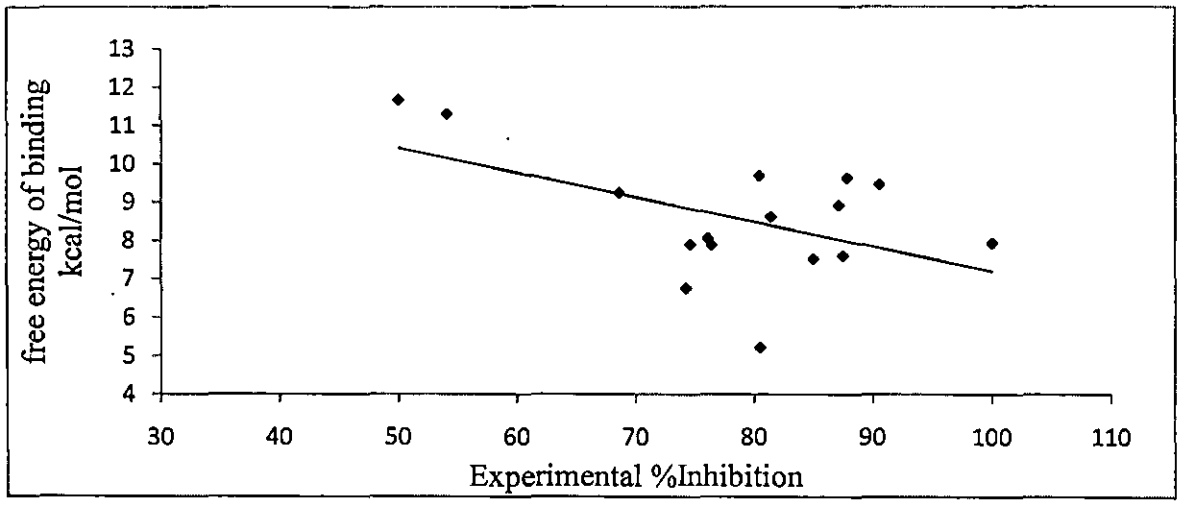

Figure 4. Correlation graph between free energy of binding and Experimental % Inhibition of training set

The values of binding free energy together with their predicted activity of designed set are given in Table 10.

Table 10. Activity of designed molecules and their binding energy with inhibitors

Compound	**Predicted %Inhibition at μM[a] HT-29 (Model 4)**	**Binding Energy (kcal/mol)**
3a	56.43	-7.73

Compound	**Predicted %Inhibition at μM[α] HT-29 (Model 4)**	**Binding Energy (kcal/mol)**
3b	70.49	-7.91
3c	79.48	-6.74
3d	73.78	-7.74
3e	74.15	-7.47
3f	70.01	-7.65
3g	98.27	-7.36
3h	87.48	-7.75
3i	75.85	-7.81
3j	78.89	-8.24
3k	67.38	-8.17
3l	61.51	-7.52
3m	81.32	-8.55
3n	71.16	-9.70
3o	57.01	-9.46
3p	54.38	-9.63
3q	21.79	-9.16
3r	66.65	-9.24
3s	83.65	-9.24
3t	75.80	-9.75
3u	55.64	-10.61
3v	60.48	-10.01
3w	73.62	-10.61
3x	74.83	-9.39
3y	61.23	-7.75
3z	106.75	-8.57
4a	71.52	-7.65

Compound	**Predicted %Inhibition at μM[α] HT-29 (Model 4)**	**Binding Energy (kcal/mol)**
4b	138.96	-8.56
4c	65.79	-8.47
4d	110.59	-8.26
4e	111.02	-5.69
4f	83.94	-7.86
4g	30.36	-11.79
4h	80.09	-9.50
4i	29.22	-9.59

The snapshot of docked compound 4a with the receptor protein is presented in Figure 5.

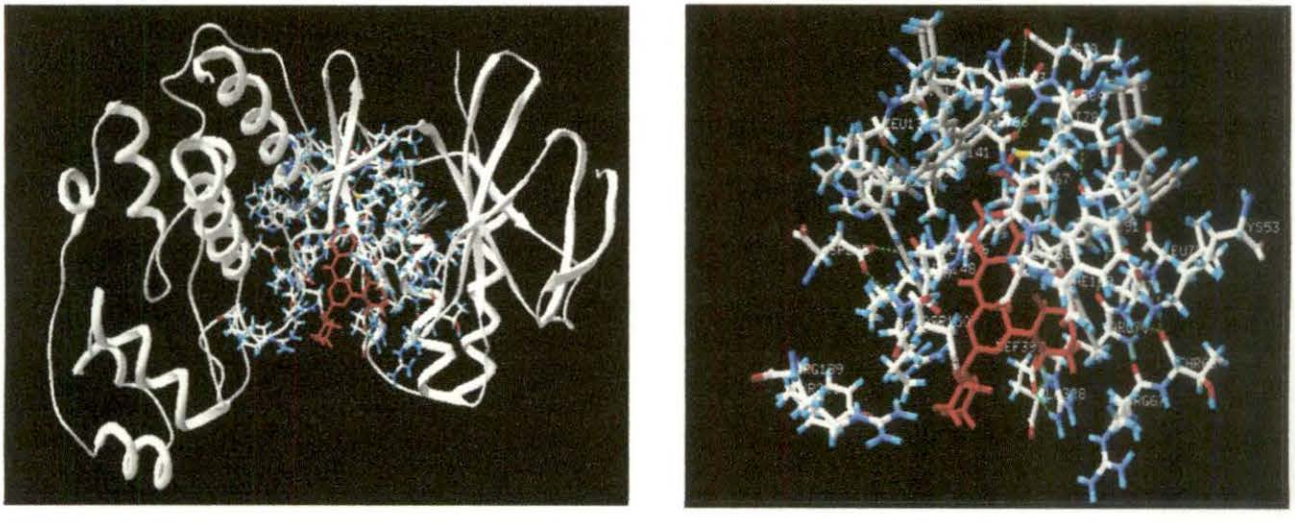

Figure 5. (A) Ribbon structure of p38 MAP kinase docked with 2,*N*,*N*-dimethyl-*N*' bis(4,6-morpholin-4-yl-1,3,5-triazin-2-yl)benzene-1,4-diamine; (B) protein with side chain with docked ligand

The triazine derivatives and their inhibition activities to HT-29 cell are depicted in Table 5. Tris (N-morpholino)-1,3,5-triazine have no inhibition activities to HT-29 cells(12). The

mono (N-morpholino) -1,3,5-triazines exhibited higher inhibitory acvtivities against HT-29 cells than their corresponding bis (N-morpholino)-1,3,5 triazine derivatives.

It was seen from our study that the compounds 3c, 3g, 3h, 3m, 3s, 4b, 4f, 4d, 4h, 4e show very high inhibition activities as predicted by our regression equation 8, whereas the compounds 3a, 3o, 3p, 3q, 3u, 4g, 4i exhibit low inhibitory activities. Rest of the molecules in Table 10 has moderate inhibition activities. Thus, from our study it seems that the compounds 3c,3g,3h,3m,3s,4b,4f,4d,4h,4e could be candidates for good inhibitors.

It is observed that all the compounds which shows high activity has at least one morpolino ring and absence of morpholino ring reduces activity value. We designed tris (anilino)-1, 3, 5-triazine (4g) and calculated their activity using our regression model, the predicted value is very low. Therefore presence of one morpholino unit plays significant role in the inhibition activities of the HT-29 cells and it is observed that the presence of three morphilino groups reduces the activity markedly. From our study it was seen that presence of three anilino group also reduces the activity markedly (4g) Replacement of one anilino group by one morpholino group enhances the activity (1p).

It may be concluded that presence of morpholino/anilino ring is essential for the activity of triazinederivates which are MAP kinase inhibitor and insertion of pyrimidine ring in triazine scaffold gives very high predicted activity as evident by compounds 4b, 4d, 4e, 4f, 3z (Table 8).

8.4: References

1. Cohen P (1997) The search for physiological substrates of MAP and SAP kinases in mammalian cells. *Trends. Cell Biol. 7*: 353–361.

2. Ip YT and Davis RJ (1998) Signal transduction by the c-Jun N-terminal kinase.(JNK): from inflammation to *development. Curr. Opin. Cell Biol.*, **10**: 205–219.

3. Davis RJ (1998) Signal transduction by the c-Jun N-terminal kinase (JNK): from inflammation to development. *Curr. Opin. Cell Biol.***10**: 205–219.

4. Kyriakis JM, Avruch J (2001) Mammalian mitogen-activated protein kinase signal transduction pathways activated by stress and inflammation. *Physiol Rev.***81**: 807-69

5. Obrero M, Yu DV, Shapiro DJ (2002) Estrogen receptor-dependent and estrogen receptor-independent pathways for tamoxifen and 4-hydroxytamoxifen-induced programmed cell death. *J Biol Chem.,277*: 4569-5703

6. Mandlekar S, Yu R, Tan TH, Kong AN (2000) Activation of caspase-3 and c-Jun NH2-terminal kinase-1 signaling pathways in tamoxifen-induced apoptosis of human breastcancer cells. *Cancer Res.*,**60**: 5995-6000.

7. Mandlekar S, Kong AN (2001) Mechanisms of tamoxifen-induced apoptosis. *Apoptosis.,6*, 469-77.

8. Wolf DM, Jordan VC, William L (1993) McGuire Memorial Symposium. Drug resistance to tamoxifen during breast cancer therapy. *Breast Cancer Res Treat,27*: 27-40.

9. Moon HS, Jacobson EM, Khersonsky SM, Luzung MR, Walsh DP (2002) *J.Am. Chem. Soc.,124*, 11608.

10. Leftheris K, Ahamed G, Chan R, Dyckman AJ, Hussain Z (2004) The discovery of orally active triaminotriazine aniline amides as inhibitors of p38 MAP kinase.*J. Med. Chem.*, *47*: 6283.

11. Baindur N, Chanda N, Brandt BM, Asgari D, Patch RJ (2005) *J. Med. Chem.*,*48*: 1717.

12. Mingfang Zheng, ChenghuiXu, Jianwei Ma, Yan Sun, Feifei Du, Hong Liu, Liping Lin, Chun Li, Jian Ding, Kaixian Chen and Huliang Jiang : Synthesis and antitumor evaluation of a novel series of triaminotriazine derivatives : *Bioorganic & Medicinal Chemistry* ,**2007**,*15*, 1815-1827.

13. Livingstone DJ (2000)The characterization of chemical structures using molecular properties. A survey.*J ChemInfComput Sci.*, **40**:195-209.

14. Ivanciuc O (2003) Graph Theory in Chemistry. In: *Handbook of Chemoinformatics*, Ed.: J. Gasteiger. Wiley-VCH. 103-138.

15. Ivanciuc O (2003) Topological Indices. In: *Handbook of Chemoinformatics*, Ed.: J.Gasteiger. Wiley-VCH. 981-1003.

16. Ivanciuc O, Balaban AT (1999) In Topological Indices and Related Descriptirs in QSAR and QPSR; J. Devillers and A.T. Balaban, Eds.; *Gordon and Breach Science Publishers*. The Netherlands. 59-167.

17. Shanon CE (1948) A mathematical theory of Communication. *Bell Syst. Tech.J.*, *27*: 379-423.

18. Basak SC, Roy AB,Ghosh JJ (1979) Study of Structure-Function Relationship of Pharmacological and Toxicological Agents Using Information Theory. *In*

proceeding of the llnd International conference on mathematical modeling, University of Missouri at Rolla. 851-856.

19. Basak SC and Magnuson VR (1983) Molecular Topology and Narcosis. A Quantitative Structure-Activity Relationship (QSAR) Study of Alcohols Usins Complementary Information Content, Arzneimittle-Froschung, *Drug Research.* 501-503.

20. MOPAC2007, James J. P. Stewart, Stewart Computational Chemistry, Colorado Springs, CO, USA, http://Open MOPAC.net, 2007.

21. http//www.seanet.com/~mthompson/Arguslab.

22. Pargellis C, Gilmore L, Graham AG, Grob PM, Hickey ER (2002)Inhibition of P38 Map-Kinase by utilizing a Novel Allosteric Binding State. *J Regan Nat. Struct. Biol.*, **9**: 268-272.